5672 *Macromolecules* **2010**, *43*, 5672–5678
DOI: 10.1021/ma100770t

Macromolecules
ARTICLE

Bio-Sourced Networks from Thermal Polyaddition of a Starch-Derived α-Azide-ω-Alkyne AB Monomer with an A_2B_2 Aliphatic Cross-linker

Céline Besset,[†] Julien Bernard,[†] Etienne Fleury,*[,†] Jean-Pierre Pascault,*[,†] Philippe Cassagnau,[†] Eric Drockenmuller,[†] and Roberto J. J. Williams[‡]

[†]*Université de Lyon, INSA-Lyon, Université Claude Bernard Lyon 1, Ingénierie des Matériaux Polymères (UMR-CNRS 5223) F-69621 Villeurbanne Cedex (France), and* [‡]*Institute of Materials Science and Technology (INTEMA), University of Mar del Plata and National Research Council (CONICET), J.B. Justo 4302,7600 Mar del Plata (Argentina)*

Received April 9, 2010; Revised Manuscript Received May 27, 2010

ABSTRACT: A starch-derived α-azide-ω-alkyne 1,4:3,6-dianhydrohexitol AB monomer and a novel symmetrical heterofunctional A_2B_2 aliphatic cross-linker, i.e., 2,2-bis(azidomethyl)-1,3-bis(*O*-propargyl) propanediol, were copolymerized at various molar ratios to generate biosourced networks through thermal 1,3-dipolar Huisgen polyaddition. The investigation of the cross-linking reactions through DSC analyses confirmed the highly exothermic character of the azide/alkyne cycloaddition ($\Delta H_{(total)} = 232 \pm 5$ kJ/mol of functional groups of type A or B) and as predicted clearly underlined a one-to-one relationship between the glass transition temperature and the conversion. Experimental values of conversion at the gel point estimated from DSC and rheological measurements deviated significantly from the ideal main-field theory of network formation. On the basis of statistical calculations, this behavior was assigned to the occurrence of intramolecular cyclizations during the network formation. Although a significant fraction of intramolecular cycles was generated during the curing process, the AB + A_2B_2 thermal 1,3-dipolar Huisgen polyaddition strategy afforded relatively high glass transition temperature polytriazole networks ($T_g \geq 140$ °C) using versatile processing conditions and in the absence of additives.

1. Introduction

Whereas the Huisgen 1,3-dipolar cycloaddition between alkynes and azides has been known for decades,[1] the recent finding of Sharpless and Meldal that Cu(I) species efficiently catalyzes the exclusive formation of 1,4-disubstituted 1,2,3-triazoles has drastically rejuvenated this chemical reaction and its application to a broad variety of fields exploiting robust, orthogonal and efficient chemical pathways.[2−4] Thus, the copper catalyzed azide−alkyne cycloaddition (CuAAC), also coined as "click chemistry", has aroused much interest among researchers because of its remarkable features such as high yield, mild reaction conditions, functional tolerance, and simple product isolation. Particularly, CuAAC has been widely applied to the efficient construction and functionalization of a broad array of tailored macromolecular materials such as linear, block and star-like copolymers, macrocycles, polymer bioconjugates, dendrimers and hyperbranched materials as well as functionalization of 2D or 3D organic and inorganic substrates.[5−10]

CuAAC has also been particularly beneficial to the design of a broad array of cross-linked polymer materials such as degradable networks, liquid crystal gel networks or hydrogels with tunable mechanical properties by step growth polymerization processes.[11−19] Indeed, triazole cross-linking knots are chemically robust to environmental conditions like oxidation or hydrolysis, and the resulting networks display advantageous properties for high-performance metal coatings, adhesives or novel binders for high energy explosive and propellant materials.[20−22]

For instance, polytriazole networks were prepared from multivalent di-, tri-, and tetraazides and alkynes directly deposited on the metal surface.[23,24] From a practical point of view, such materials are expected to be used as corrosion inhibitors or adhesives on copper or copper based substrates. In these studies, the substrate was assumed to provide the catalytic species involved in the CuAAC curing process. Thermosetting polymers based on A_2 + B_4 or A_4 + B_2 (A = azide and B = alkyne) thermosetting polymers were found to exhibit unusually high glass transition temperatures (T_g) with respect to the curing temperature (up to 60 °C higher than the curing temperature). This behavior was observed for curing temperatures ranging from 20 to 100 °C. It was also shown that the films generated between the two plates continue to react after the T_g of the network reached the curing temperature, showing some local mobility, in spite of the polymer being in the glassy state.[25] Other authors have applied the thermal 1,3-dipolar Huisgen polyaddition to the preparation of cross-linked polytriazole matrices suitable for advanced composite materials.[26−29] For instance, A_2 or A_3 aromatic azides and B_2 or B_4 aromatic alkynes have been prepared, precured at 70−80 °C and subsequently postcured at temperatures up to 200 °C. The kinetics of the curing process, gel times (t_{gel}), T_g and mechanical properties were measured. In this case, the T_g values of the cured products at different stages of the reaction were also ca. 50 °C higher than the precuring temperatures.[26] Mechanical properties of composites prepared with glass fibres and polytriazole matrices obtained from an A_3 + B_2 reactive mixture have also been investigated.[29]

We have previously studied the CuAAC step growth polymerization of A_2 + B_2 or self-reacting AB monomers and the structure/properties relationship of the resulting linear polytriazoles.[30,31] In a recent paper,[32] we described the preparation of α-azide-ω-alkyne AB monomers with controlled stereochemistry from 1,4:3,6-dianhydrohexitols. 1,4:3,6-dianhydrohexitols, especially isosorbide

*Corresponding authors. E-mail: (J.-P.P.) jean-pierre.pascault@insa-lyon.fr; (E.F.) etienne.fleury@insa-lyon.fr.

 Published on Web 06/02/2010

and isomannide, can be straightforwardly synthesized through sequential hydrogenation and dehydration of starch-derived D-glucose and D-mannose, respectively.[33] The polyaddition of these α-azide-ω-alkyne AB monomers by CuAAC in solution or by catalyst and solvent-free 1,3-dipolar Huisgen cycloaddition was investigated in detail. It was shown that thermal polyaddition in bulk provides polytriazoles with enhanced solubility, higher molar mass and thermal properties comparable to those obtained by CuAAC in solution. Besides an appreciable simplification of the processing conditions, the influence of monomer stereochemistry and polyaddition regioselectivity on the physicochemical properties of the resulting materials was discussed.

Extrapolating from our previous work, we report in the present paper a comprehensive study on the generation of high T_g biosourced networks from thermal Huisgen polyaddition of a starch-derived α-azide-ω-alkyne 1,4:3,6-dianhydrohexitol **AB** stereoisomer in the presence of a tailor-made symmetrical $\mathbf{A_2B_2}$ cross-linker. Using differential scanning calorimetry (DSC) and rheological measurements in combination with statistical calculations, we investigate herein the formation of polytriazole networks and the physicochemical properties of the resulting materials at different $\mathbf{AB/A_2B_2}$ ratios and polymerization temperatures.

2. Experimental Section

Materials. 2,2-Bis(bromomethyl)-1,3-propanediol (Aldrich, 98%), sodium hydride (Aldrich, 60% dispersion in mineral oil), propargyl bromide (Aldrich, 80 wt % in toluene), 18-*crown*-6 (Aldrich, 99%), sodium azide (Alfa Aesar, 99%), dimethylformamide (DMF, Aldrich, 99%), dimethyl sulfoxide-d_6 (DMSO-d_6, Aldrich, 100%) were used as received. The synthesis of the 1,4:3,6-dianhydro-5-azido-2-O-propargyl-5-deoxy-D-sorbitol having respectively a S and R absolute configuration for carbons 2 and 5 (**AB**) was performed using a synthetic pathway described earlier.[32]

Synthesis of the $\mathbf{A_2B_2}$ Cross-Linker. *Synthesis of 2,2-Bis(azidomethyl)-1,3-propanediol,* $\boldsymbol{A_2R}$. A suspension of 2,2-bis(bromomethyl)-1,3-propanediol (15 g, 57 mmol) and sodium azide (15 g, 231 mmol) in dimethylformamide (200 mL) was heated at 120 °C for 24 h. (*Caution! Sodium azide is highly toxic by inhalation and ingestion, yields highly toxic hydrazoic acid under acidic conditions, and may react with lead or copper to form highly explosive metal azides*). Excess sodium azide was filtered and the solution was diluted with dichloromethane (500 mL) and washed with water (2 × 400 mL). The combined organic phases were dried with $MgSO_4$, filtered and partially concentrated under vacuum giving $\mathbf{A_2R}$ (9.8 g, 92%) as a solution in 50 mL of dimethylformamide. ^{1}H NMR (C_2D_6SO): δ 4.74 (t, 2H, J = 4.9 Hz, OH), 3.27−3.32 (m, 8H, C**H**$_2$OH, C**H**$_2$N$_3$). ^{13}C NMR (C_2D_6SO): δ 60.0 (**C**H$_2$OH, 2C), 51.2 (**C**H$_2$N$_3$, 2C), 45.6 (**C**q, 1C).

Synthesis of 2,2-Bis(azidomethyl)-1,3-bis(O-propargyl)-propanediol, $\boldsymbol{A_2B_2}$. NaH (8.5 g, 211 mmol) was added to a solution of diazide $\mathbf{A_2R}$ (9.8 g, 53 mmol) in 150 mL of dimethylformamide maintained at 0 °C under argon. After hydrogen was entirely emitted, propargyl bromide (23.5 mL, 211 mmol) and 18-*crown*-6 (0.50 g, 1.4 mmol) were added and the mixture was stirred for 12 h at room temperature. After neutralization of residual NaH by distilled water (30 mL), the solvents were evaporated under reduced pressure and the residue was extracted with dichloromethane (3 × 500 mL). The organic layer was dried with $MgSO_4$, filtered and concentrated under reduced pressure. The residue was purified by column chromatography on silica gel, eluting with a 85:15 mixture of petroleum ether and ethyl acetate giving after evaporation of the solvents $\mathbf{A_2B_2}$ as a yellow liquid (11.7 g, 85%). ^{1}H NMR (C_2D_6SO): δ 4.15 (d, 4H, J = 2.4 Hz, OC**H**$_2$C≡CH), 3.46 (t, 2H, J = 2.4 Hz, CH$_2$C≡C**H**), 3.33−3.36 (m, 8H, C**H**$_2$O, C**H**$_2$N$_3$). ^{13}C NMR (C_2D_6SO): δ 79.5 (OCH$_2$**C**≡CH, 2C), 77.2 (OCH$_2$C≡**C**H, 2C), 68.2 (**C**H$_2$O, 2C), 58.0 (O**C**H$_2$C≡CH, 2C), 51.4 (**C**H$_2$N$_3$, 2C), 44.2 (**C**q, 1C). HRMS: m/z calcd for $C_{11}H_{14}N_6O_2$ (m/z + H), 263.1256; found, 263.1256.

Synthesis of the Polytriazole Network. Different $\mathbf{AB/A_2B_2}$ mixtures (3:1, 2:1, 1:1, 1:2, and 0:1 molar ratios) were mixed at room temperature in a vial. Thermal curing of these reactive formulations were performed under different processing conditions, i.e., in bulk, in thin films, under a hot press, in DSC capsules, or in a cone and plate rheometer. In every case, the resulting polytriazole networks were obtained quantitatively as a slightly brown glassy solid.

Analytical Methods. NMR spectra were recorded on a Bruker AC spectrometer at 300 MHz for ^{1}H and 75 MHz for ^{13}C. High resolution mass spectrometry (HRMS) were recorded on a Thermo Finnigan spectrometer at the Centre de Spectrométrie de Masse de l'Université Claude Bernard Lyon 1. Differential scanning calorimetry (DSC) was performed under nitrogen using a DSC 2920 (TA Instruments).

DSC Monitoring of the Curing Process. Initially, several DSC capsules containing ca. 5 mg of $\mathbf{AB/A_2B_2}$ mixtures were sealed off under ambient conditions and heated in the DSC apparatus from −90 to 260 °C at a heating rate of 10 °C/min to obtain the initial glass transition temperature (T_{g0}) and total enthalpy of reaction (ΔH_∞). Following each initial scan, a second dynamic scan at 10 °C/min was performed to evaluate the glass transition temperature of the resulting polymer ($T_{g\infty}$). T_g was taken as the midpoint of the heat capacity change. ΔC_{p0} and $\Delta C_{p\infty}$ values were obtained averaging 5 runs. Also, capsules were preheated in an oven at isothermal temperatures of 80 or 100 °C during times ranging from 10 to 240 min before being quenched in liquid nitrogen and directly analyzed by DSC to access $T_g(t)$ of the formed polytriazoles and residual enthalpy of reaction, $\Delta H(t)$.

The conversion of reactive groups, x, at time, t, is given by

$$x = 1 - \Delta H(t)/\Delta H_\infty \quad (1)$$

ΔH_∞ being the enthalpy of the reaction (heat of reaction of initial monomer mixture) and $\Delta H(t)$ the residual enthalpy of reaction at time t.

Rheology. Viscoelastic properties were measured under a stream of dry nitrogen at constant temperature, using a Rheometrics mechanical spectrometer (RMS800). Rheological kinetics were obtained in real time with a parallel-plate geometry (o.d. = 25 mm). The thickness of the sample (gap of the parallel-plate) was ca. 1 mm. The parallel-plate system was preheated to the temperature of the experiment. As explained below, the study of the dynamic mechanical behavior at the gel point requires the measurement of both loss and storage moduli at several frequencies. Therefore, it is important to consider the mutation number (N_{mu}) criterion which gives the relative changes of the measured variables (G' or G'') during the sampling time.[34] For our experiments, N_{mu} was lower than 0.1 in the frequency range $1 \le \omega(\text{rad/s}) \le 100$. The measurements were then performed at several pulse rates of ca. 100, 46, 21, 10, 5, and 1 rad/s.

Winter and Chambon showed that the frequency dependence of G' and G'' can be represented by a power law over a large angular frequency range:[35]

$$G'(\omega) \propto G''(\omega) \propto \omega^\Delta \quad (2)$$

with ω the frequency and Δ the relaxation exponent. This fact can be used to determine (t_{gel}) from the crossover of the tan δ curves at various angular frequencies since

$$G''/G' = \tan\delta = \tan(\pi\Delta/2) \quad (3)$$

It can be noted that the measurements are performed at several frequencies, consequently take a finite time and thus are not obtained at the same reaction time. However this experimental aspect is not restrictive in the present objective as t_{gel} is determined

Scheme 1. Syntheses of the AB Monomer and A_2B_2 Cross-Linker

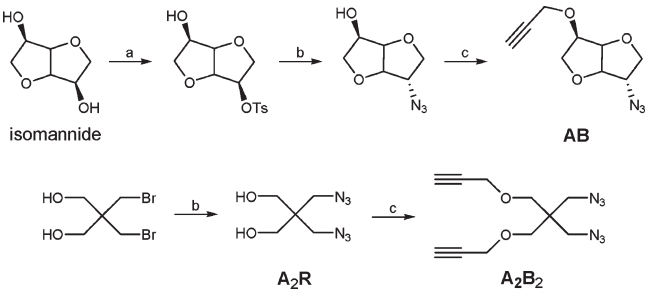

from the frequency-invariance of tan $\delta = G''/G'$. This experimental method represents the most powerful method to have an easy access to an accurate value of t_{gel}.

3. Results and Discussion

Syntheses of the AB Monomer and the A_2B_2 Cross-Linker. The α-azide-ω-alkyne dianhydrohexitol **AB** monomer used in this work (S and R absolute configuration for carbons 2 and 5) was obtained as previously described from isomannide using a three-step synthetic pathway (Scheme 1). This monomer was chosen as its multistep synthesis provided higher yields compared to the other stereoisomers.[32] An alternative two-step procedure without protection of the alcohol groups was involved in the preparation of the $\mathbf{A_2B_2}$ cross-linker. It must be underlined that the preparation of such symmetrical heterofunctional $\mathbf{A_2B_2}$ has not been addressed previously. Indeed, polytriazole networks are generally obtained from bicomponent systems involving $\mathbf{A}_n$ or $\mathbf{B}_n$ multifunctional derivatives. In a first step, nucleophilic substitution of the two bromides from commercial 2,2-bis-(bromomethyl)-1,3-propanediol by sodium azide yielded 2,2-bis(azidomethyl)-1,3-propanediol ($\mathbf{A_2R}$) in 92% yield. Then, alkylation of the remaining hydroxyl groups by propargyl bromide was performed at room temperature to avoid any undesirable step growth polymerization, yielding 2,2 bis(azidomethyl)-1,3-bis(*O*-propargyl) propanediol ($\mathbf{A_2B_2}$) in 85% yield. After purification by column chromatography, the $\mathbf{A_2B_2}$ cross-linker was characterized by HRMS, ^{1}H and ^{13}C NMR spectroscopy before being stored at −20 °C, a temperature below which no traces of coupling products could be observed by ^{1}H NMR after several months of storage.

Thermal Curing Behavior. The conversion of initial alkyne and azide functionalities to 1,4- and 1,5-disubstituted 1,2,3-triazoles through thermal 1,3-dipolar cycloaddition of different formulations, i.e. pure **AB** and $\mathbf{A_2B_2}$ reactants and their 3:1, 2:1, 1:1, and 1:2 molar mixtures, was initially investigated by DSC at a heating rate of 10 °C/min. Typically, a first heating scan was performed from −90 to 260 °C to determine T_{g0}, ΔC_{p0} and ΔH_{total} for a given formulation (Figure 1). A second heating run of the cured sample subsequently afforded $T_{g\infty}$ and $\Delta C_{p\infty}$ values after full conversion of the reactive groups. T_g, ΔC_p, and ΔH_{total} values obtained for the six formulations studied herein are given in Table 1. The shape of the DSC curves was similar for all $\mathbf{AB}/\mathbf{A_2B_2}$ formulations. Typically, the thermal 1,3 dipolar cycloaddition starts at ca. 60 °C and ends at ca. 250 °C while the peak of the exothermal reaction (T_p) is observed at 140−150 °C (at a constant heating rate of 10 °C/min). Similar values of T_p have been reported in the literature for thermally cured polytriazole networks.[26−29]

ΔC_{p0} and T_{g0} of the pure monomers were very close, a fact that led to an almost constant value of ΔC_{p0} and T_{g0} for the different mixtures of **AB** and $\mathbf{A_2B_2}$. Except for the homopolymerization of $\mathbf{A_2B_2}$, very close values of ΔH_{total} (average ΔH_{total} of 232 ± 5 kJ/mol func) were observed for the different $\mathbf{AB}/\mathbf{A_2B_2}$ formulations. These values are in good agreement with literature data (given in J/g in the cited references), i.e., 254 kJ/mol func for a $A_2 + B_4$ system,[26,27] 230 kJ/mol func for a $A_3 + B_2$ system[29] and 205 kJ/mol func for a highly cross-linked $A_3 + B_4$ system.[28] It has to be pointed out that these values are much higher than those observed for other reactive systems such as epoxies, cyanate-esters or bismaleimides for which ΔH_{total} is generally in the range of 100−110 kJ/mol func.[36] The highly exothermic nature of the azide−alkyne cycloaddition reaction thus justifies the application of such reactive formulations in rocket propellant binder compositions[20] and could explain how polytriazole networks with T_g values as high as 60 °C above the curing temperature can be generated. Similar to the $A_3 + B_4$ system cited above, the particularly low value of ΔH_{max} observed in the case of $\mathbf{A_2B_2}$ homopolymerization (207 ± 5 kJ/mol func) suggests that full conversion cannot be achieved because of network steric hindrance in the latest stages of the cross-linking reaction. From the ratio of reaction heats $\Delta H_{max}/\Delta H_{total}$ the maximum conversion of functional groups for the $\mathbf{A_2B_2}$ homopolymerization was estimated to be ca. 87%.

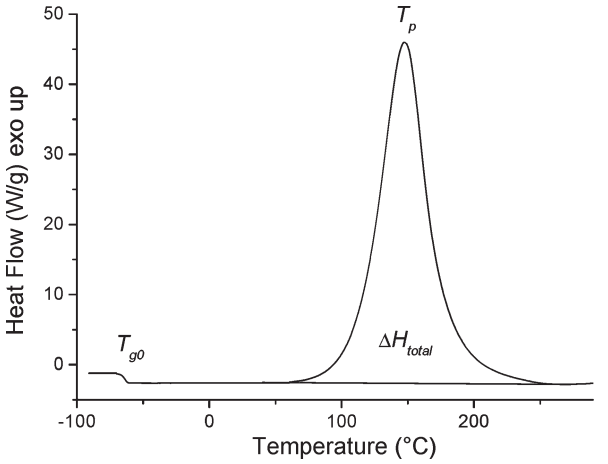

Figure 1. Evolution of DSC traces with temperature during the thermal curing of a 1:1 mixture of $\mathbf{AB}/\mathbf{A_2B_2}$ in bulk at a heating rate of 10 °C/min.

Glass Transition Temperature, T_g as a Function of Conversion, x. The following equation can be used to describe the evolution of T_g as a function of x:[37]

$$[T_g(t) - T_{g0}]/(T_{g\infty} - T_{g0}) = \lambda x/[1 - (1 - \lambda)x] \quad (4)$$

with $T_g(t)$ the glass transition temperature of the polymerization media after a curing step for a time t (or a given conversion), $\lambda = \Delta C_{p\infty}/\Delta C_{p0}$, T_{g0} and $T_{g\infty}$ being extracted from Table 1. All the parameters of this equation can be straightforwardly measured by DSC. The evolution of $T_g(t)$ as a function of x was thus monitored after an isothermal curing for a given time for all formulations. $T_g(t)$ values predicted from eq 4 and experimental $T_g(t)$ versus conversion plots for the isothermal curing of a 1:1 ratio $\mathbf{AB}/\mathbf{A_2B_2}$ mixture are given in Figure 2.

The same procedure was also applied to the homopolymerization of $\mathbf{A_2B_2}$ (Figure 3). In this case, the predicted evolution of $T_g(t)$ is described by eq 5 which applies to partially reacted networks:[38]

$$[T_g(t) - T_{g0}]/(T_{gmax} - T_{g0}) = \lambda' x'/[1 - (1 - \lambda')x] \quad (5)$$

Table 1. DSC Results for Different AB/A_2B_2 Formulations Thermally Cured by Catalyst- and Solvent-Free Azide−Alkyne Cycloaddition

AB/A_2B_2 molar ratio	T_{g0} (°C)	ΔC_{p0} (J/(g/K))	ΔH_{total} (kJ/mol func) ± 5 kJ/mol	$T_{g\infty}$ (°C)	$\Delta C_{p\infty}$ (J/(g/K))
1:0	−72	0.115	237	124	0.061
3:1	−68	0.121	231	143	0.059
2:1	−70	0.124	233	149	0.062
1:1	−69	0.116	227	158	0.061
1:2	−70	0.115	229	172	0.058
0:1	−70	0.110	207[a]	200[a]	0.062[a]

[a] The particularly low value of ΔH suggests that full conversion was not achieved in the case of $\mathbf{A_2B_2}$ homopolymerization (~87%, see text). Consequently, the terms ΔH_{max} and T_{gmax} will be used instead of $T_{g\infty}$ and ΔH_{total}.

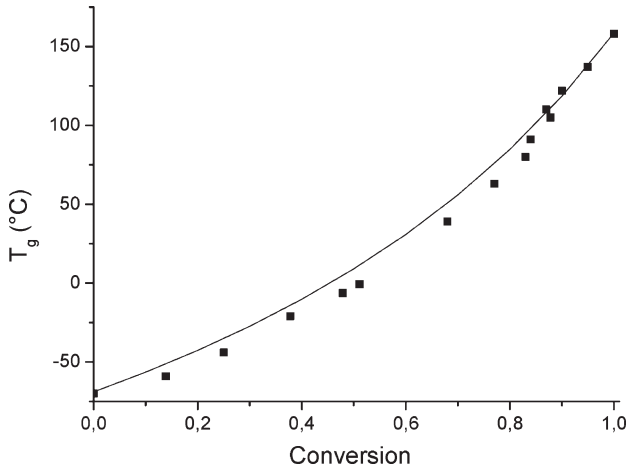

Figure 2. Evolution of T_g as a function of conversion for the thermal curing of a 1:1 mixture of **AB**/$\mathbf{A_2B_2}$. Experimental values were obtained by DSC after isothermal curing of the sample for different reaction times and temperatures. The solid line is the prediction resulting from eq 4.

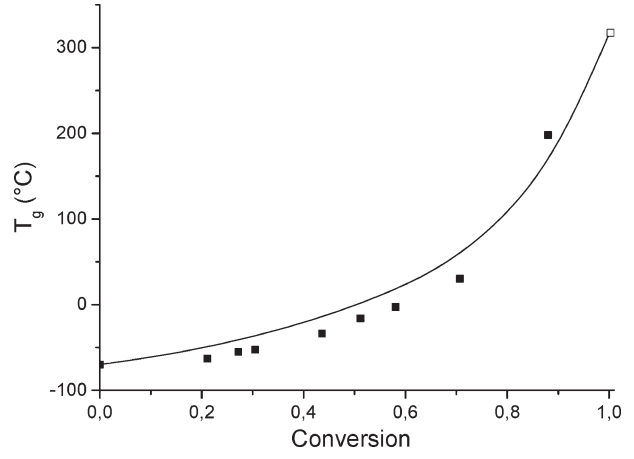

Figure 3. Evolution of T_g as a function of conversion for the thermal curing of the $\mathbf{A_2B_2}$ cross-linker. Solid squares are experimental values obtained by DSC after isothermal curing of the sample for different reaction times and temperatures. Open square data is the predicted $T_{g\infty}$ value (316 °C) obtained from eq 5 for $x = 1$. The solid line is the prediction resulting from eq 5.

with $x' = x/x_{max}$, $\lambda' = \Delta C_{pmax}/\Delta C_{p0}$. x_{max}, ΔC_{pmax}, and T_{gmax}, the maximum values obtained after curing the pure $\mathbf{A_2B_2}$ cross-linker (87% of converted functional groups).

As illustrated by Figure 2 and 3, a very satisfactory agreement between the model and the experimental results was observed for every formulation. This one-to-one relationship between T_g and x has been described for many thermosetting polymers[36] and confirms that from the network formation point of view, the azide/alkyne cycloaddition reaction presents similar characteristics as other cross-linking reactions.

Table 2. Characteristics at the Gel Point for Different AB/A_2B_2 Ratios Thermally Cured by Catalyst and Solvent Free Azide−Alkyne Cycloaddition

AB/A_2B_2 mol ratio	3:1	1:1	1:1
temperature (°C)	100	100	80
t_{gel} (s)	1610	700	3520
tan δ	2.4	2.6	2.5
Δ^a	0.75	0.77	0.76
$x_{gel}{}^b$	0.72	0.57	0.57
theoretical $x_{gel}{}^c$	0.56	0.43	0.43

[a] Calculated from eq 3). [b] Calculated from $\Delta H(t)$ using eq 1. [c] Calculated from eq 6 (Appendix 1).

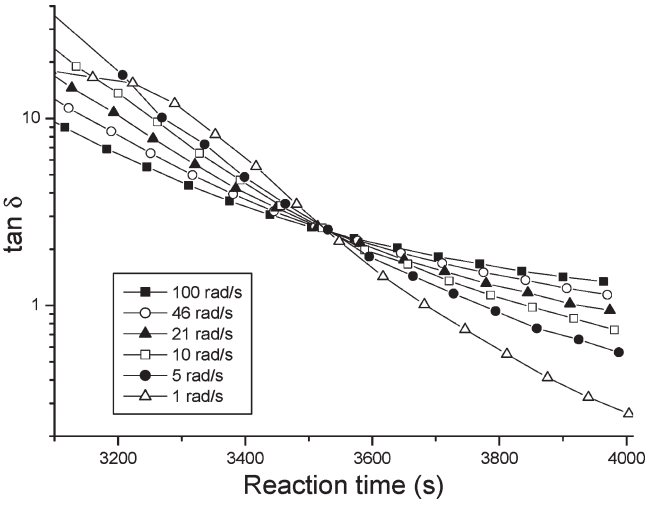

Figure 4. Evolution of tan δ at different applied frequencies as a function of reaction time for the curing of a 1:1 mixture of **AB**/$\mathbf{A_2B_2}$ at 80 °C.

In contrast to the thermal 1,3-dipolar polyaddition of **AB** which affords linear polytriazoles with T_g equal to 124 °C, the copolymerization of **AB** and $\mathbf{A_2B_2}$ resulted in the preparation of biosourced polytriazole networks with T_g ranging from 143 °C for an **AB**/$\mathbf{A_2B_2}$ ratio of 3:1, to 172 °C for an **AB**/$\mathbf{A_2B_2}$ ratio of 1:2 while $\mathbf{A_2B_2}$ homopolymerization generated networks with a T_g of 200 °C. As expected, the cross-linker concentration and thus the cross-link density strongly impacted the final value of T_g. A full understanding of the evolution of T_g is however rather complex due to the copolymer effect accounting for the different chemical structures of the **AB** and $\mathbf{A_2B_2}$ components as well as the topological properties of the resulting networks.

Gelation Behavior of the Reactive Mixtures. The formation of the polytriazole networks was investigated by rheological analyses.[39] The values of t_{gel} were precisely determined for 1:1 and 3:1 **AB**/$\mathbf{A_2B_2}$ mixtures at 80 and 100 °C using isothermal multiwave tests, t_{gel} corresponding to the cross-over point of the tan δ versus time curves (Table 2). As an example, the tan δ versus time plots of a 1:1 **AB**/$\mathbf{A_2B_2}$ mixture at different applied frequencies at 80 °C are given in Figure 4.

Depending on the $\mathbf{A_2B_2}$ concentration and curing temperatures, t_{gel} values ranging from 700 to 3520 s were obtained. The tan δ values in the range of 2.4−2.6 were observed leading to values of relaxation exponent (Δ = 0.75−0.77, calculated from eq 3) close to that of the percolation model ($\Delta \sim 0.70$).[23] Δ appeared to be independent of the cross-linker concentration and the curing temperature.

Conversions at the Gel Point, x_{gel}. The samples generated from the rheological analyses were quenched in liquid nitrogen at the gel point in order to assess conversions at the gel point (x_{gel}), establish a comparison with the theoretical value of the conversion (at the gel point) for an ideal network and investigate the network characteristics under different processing conditions. Theoretical values of x_{gel} reported in Table 2 were calculated from eq 6, which was developed by an ideal statistical model using the mean-field approach (see details of the calculation in Appendix 1).

$$x_{gel} = (1+2r)/(1+6r) \quad (6)$$

where $1/r$ is the $\mathbf{AB}/\mathbf{A_2B_2}$ molar ratio

The DSC analyses of the samples allowed to determine residual $\Delta H(t_{gel})$ and then to calculate conversions at the gel point, x_{gel}. It is of interest though to note that as expected for a step growth polymerization, similar results for conversions at the gel point were obtained for the curing at 80 and 100 °C of a 1:1 $\mathbf{AB}/\mathbf{A_2B_2}$ ratio underlying the reproducibility of the experimental procedures used herein. These experimental values of x_{gel} were significantly higher than the theoretical ones (for r = 1/3, theoretical x_{gel} = 0.56 and experimental x_{gel} = 0.72; for r = 1, theoretical x_{gel} = 0.43 and experimental x_{gel} = 0.57). Since no data on a thermal 1,3-dipolar polyaddition $\mathbf{AB} + \mathbf{A_2B_2}$ system could be found in the literature, these results were compared with the work of Liu et al. dealing with a $A_2 + B_4$ system.[14] In this paper, the authors reported t_{gel} and kinetic results at different temperatures so that experimental x_{gel} could be easily estimated. Indeed, the authors reported first order kinetics valid up to conversions of ca. 0.75 (Figure 5 in ref 14) given by $dx/dt = k(1-x)$ with $\ln k\,(\mathrm{min}^{-1}) = 21 - 9060/T(\mathrm{K})$. By integration, the conversion for isothermal runs is given by $x = 1 - \exp(-kt)$. Using t_{gel} (Table 3 in ref 14), an average value of the experimental x_{gel} equal to 0.64 was determined while the theoretical value of x_{gel} was 0.58. This result clearly highlights that our $\mathbf{AB} + \mathbf{A_2B_2}$ system behaves in an analogous manner to the highly cross-linked $A_2 + B_4$ system.

The discrepancy between theoretical and experimental values of x_{gel} can be ascribed to the failure of the hypotheses used to derive the ideal model described in Appendix 1: (i) equal reactivity of functionalities present in the starting monomers, (ii) absence of substitution effects (functionalities present in partially reacted monomers keep their initial reactivity), (iii) absence of intramolecular cycles. Considering the chemical structure of the monomers developed in this work, failure to hypothesis i can reasonably be ruled out. Besides, calculations (not shown here) indicated that substitution effects can not account for the significant departure of experimental and theoretical gel conversions. As a consequence, the deviation to theoretical values of x_{gel} can probably be assigned to the formation of intramolecular cycles throughout the formation of the network. The effect of intramolecular cycles on x_{gel} has been extensively investigated in the literature.[40] A clear understanding of the influence of these cycles on x_{gel} requires to precisely evaluate the proportions of the different multifunctional species along the polymerization as well as the probability to generate intramolecular cycles. Approximate methods have been devised to solve this complex problem. In our case, a rough approximation exclusively taking into account the formation of the shortest intramolecular cycles from an **AB** monomer reacting with A and B functionalities of the same $\mathbf{A_2B_2}$ monomer was made although the formation of cycles from two $\mathbf{A_2B_2}$ monomers as well as the formation of larger cycles can not be excluded (Figure 5). We also assumed that an $\mathbf{A_2B_2}$ fragment can only incorporate one intramolecular cycle and that the fragment with two intramolecular cycles is not allowed (see details in Appendix 2). Resolution of this system yields eq 7 which gives the proportion of intramolecular cycles, $f(x_{gel})$, as a function of r and x_{gel}.

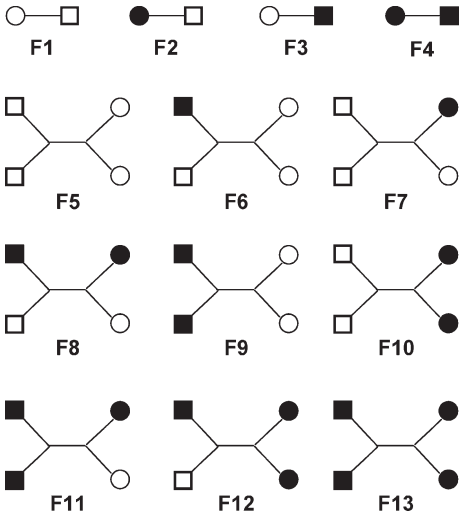

Figure 5. Scheme for different states of reaction of monomer **AB** and cross-linker $\mathbf{A_2B_2}$. See Appendix 1.

$$f(x_{gel}) = [(1+6r)x_{gel} - (1+2r)]/[4r{x_{gel}}^2(2-x_{gel})] \quad (7)$$

Using the experimental values of x_{gel}, the fraction of intramolecular cycles in $\mathbf{A_2B_2}$ species at the gel conversion was found to be 45 ± 11% for 1:1 and 3:1 $\mathbf{AB}/\mathbf{A_2B_2}$ mixtures meaning that once an **AB** monomer has first reacted with a $\mathbf{A_2B_2}$ cross-linker, there is a significantly high probability that the remaining free functionality subsequently reacts with the neighboring group of the same molecule to form a cycle and a new difunctional unit. This process can also occur by head-to-tail cyclodimerization between **AB** and $\mathbf{A_2B_2}$ species. Independently of the value determined by the approximate statistical model we can infer that the formation of a large fraction of short intramolecular cycles is necessary to account for the significant shift in the gel conversions with respect to the ideal values.

4. Conclusions

New starch-derived networks have been conveniently prepared by bulk copolymerizing a starch-derived α-azide-ω-alkyne 1,4:3,6-dianhydrohexitol **AB** monomer with an $\mathbf{A_2B_2}$ aliphatic cross-linker through thermal Huisgen polyaddition. The formation of polytriazole networks was evidenced by rheological investigations. Using samples quenched at t_{gel}, experimental conversions at the gel point were subsequently estimated by DSC. These experimental values were shown to be significantly higher than theoretical values (for r = 1/3, theoretical x_{gel} = 0.56 and experimental x_{gel} = 0.72; for r = 1, theoretical x_{gel} = 0.43 and experimental x_{gel} = 0.57) suggesting that one of the hypothesis used to derive the ideal model is not appropriate to the $\mathbf{AB}/\mathbf{A_2B_2}$ system. Relying on statistical calculations and chemical considerations, the deviation was assigned to the occurrence of intramolecular cyclizations throughout the formation of the network. Nevertheless, the thermal Huisgen

polyaddition of **AB**/$\mathbf{A_2B_2}$ afforded biosourced polytriazole networks with relatively high and tunable glass transition temperatures.

Acknowledgment. The authors gratefully acknowledge the financial support from Roquette Frères as well as Mathias Ibert and Patrick Fuertes from Roquette Frères Research Division for fruitful discussions.

Appendix 1: Ideal Network Formed by the Reaction of AB with $\mathbf{A_2B_2}$

The different states of reaction of both monomers are indicated in Figure 5; F1 represents the unreacted **AB** monomer while F5 indicates the unreacted $\mathbf{A_2B_2}$ cross-linker (A is represented by an open circle and B by an open square). The starting system has 1 mol of F1 and r moles of F5. Reacted functionalities are represented by solid circles and squares. The concentration of different fragments F1−F13 (Figure 5) may be obtained by probabilistic considerations assuming that the reactions follow an ideal path defined by the following conditions: (i) equal reactivity of functionalities present in the starting monomers, (ii) absence of substitution effects (once a functionality reacts the remaining functionalities keep their initial reactivity), and (iii) absence of intramolecular cycles in finite species.

Under these conditions, the concentration of different fragments may be expressed as a function of conversion (x) as follows:

$$\mathrm{F1} = (1-x)^2$$

$$\mathrm{F2} = x(1-x)$$

$$\mathrm{F3} = x(1-x)$$

$$\mathrm{F4} = x^2$$

$$\mathrm{F5} = r(1-x)^4$$

$$\mathrm{F6} = 2rx(1-x)^3$$

$$\mathrm{F7} = 2rx(1-x)^3$$

$$\mathrm{F8} = 4rx^2(1-x)^2$$

$$\mathrm{F9} = rx^2(1-x)^2$$

$$\mathrm{F10} = rx^2(1-x)^2$$

$$\mathrm{F11} = 2rx^3(1-x)$$

$$\mathrm{F12} = 2rx^3(1-x)$$

$$\mathrm{F13} = rx^4$$

The gel conversion may be obtained using the fragment approach.[35] The concentration of reacted A functionalities (solid circles), equal to the concentration of reacted B functionalities (solid squares), is given by $(1 + 2r)x$ as a result from the previous expressions. Because of the symmetry of the system, the average mass (W) attached to a solid circle is equal to the average mass attached to a solid square (this can be proved by making the statistical derivations taking both values as independent variables). A solid circle must be bonded to a solid square; the probability of bonding a particular fragment containing solid squares is equal to the fraction of total solid squares present in this fragment. The mass attached is equal to the mass of the fragment (M_1 for F1 to F4 and M_2 for F5 to F13) plus the mass attached to the remaining reacted solid squares and circles (W for each one of the remaining reacted functionalities). We can calculate the average mass attached to a solid circle as:

$$\begin{aligned} W = [1/(1+2r)x][&\mathrm{F3}(M_1) + \mathrm{F4}(M_1+W) + \mathrm{F6}(M_2) \\ &+ \mathrm{F8}(M_2+W) + 2\mathrm{F9}(M_2+W) + 2\mathrm{F11}(M_2+2W) \\ &+ \mathrm{F12}(M_2+2W) + 2\mathrm{F13}(M_2+3W)] \end{aligned}$$

Expressing the concentrations of fragments in terms of conversion and rearranging leads to:

$$W = (M_1 + 2rM_2)/[1+2r-x(1+6r)]$$

The gel conversion is defined by the condition that $W \rightarrow \infty$ which is attained when

$$x_{\mathrm{gel}} = (1+2r)/(1+6r)$$

This last equation was used to calculate the theoretical conversion at the gel point (x_{gel}).

Appendix 2: Gel Conversion in the Presence of Short Intramolecular Cycles

The influence of the formation of intramolecular cycles on the shift of the ideal gel conversion may be estimated by making the following hypotheses: (i) a fraction $f(x)$ of fragments F8, F11, F12, and F13 has a solid circle and a solid square connected by an F4 fragment (intramolecular bond between **AB** and $\mathbf{A_2B_2}$); this corresponds to a fraction $c(x)$ of F4 fragments present in the form of intramolecular cycles; (ii) formation of intramolecular cycles affects the connectivity of the network but does not alter the overall concentration of different fragments, calculated in a similar way than for the ideal network (e.g., the overall concentration of F4 = x^2, a fraction $c(x)x^2$ is included in intramolecular cycles while a fraction $[1 - c(x)]x^2$ forms intermolecular bonds).

Both fractions $f(x)$ and $c(x)$ can be related by the stoichiometry of the system,

$$f(x)(\mathrm{F8} + \mathrm{F11} + \mathrm{F12} + \mathrm{F13}) = c(x)x^2$$

Expressing the concentrations of fragments in terms of conversion and rearranging leads to:

$$f(x) = c(x)/r(2-x)^2$$

The concentration of solid circles or solid squares (each type of reacted functionalities) is equal to $(1 + 2r)x$ as for the ideal case. However, in order to perform statistical calculations in the presence of cycles it is necessary to discount the concentration of solid circles or squares that are connected intramolecularly. The concentration of intramolecular bonded functionalities is equal to twice the concentration of F4 present in the form of cycles (F4 fragments bonded to a solid circle and a solid square), $2c(x)x^2$. Therefore, the concentration of solid circles or squares that allows formation of a network is given by $(1 + 2r)x - 2c(x)x^2 = (1 + 2r)x - f(x)2rx^2(2 - x)^2$.

We now want to calculate the average mass that will be extracted from the mixture of fragments when "fishing" with a solid circle. The probability of bonding a particular fragment is equal to the fraction of solid squares available to form a network, present in the particular fragment. The extracted average mass is calculated as:

$$W = \{1/[(1+2r)x - f(x)2rx^2(2-x)^2]\}\{\mathrm{F3}(M_1) + [1-c(x)]\mathrm{F4}(M_1+W) + \mathrm{F6}(M_2) + [1-f(x)]\mathrm{F8}(M_2+W) + 2\mathrm{F9}(M_2+W) + [1-f(x)]2\mathrm{F11}(M_2+2\mathrm{W}) + f(x)\mathrm{F11}(M_1 + M_2) + [1-f(x)]\mathrm{F12}(M_2+2W) + [1-f(x)]2\mathrm{F13}(M_2 + 3W) + f(x)\mathrm{F13}(M_1+M_2+W)\}$$

Expressing the concentrations of fragments in terms of conversion, $c(x)$ in terms of $f(x)$, and getting the condition for $W \rightarrow \infty$ leads to:

$$f(x_{gel}) = [(1+6r)x_{gel} - (1+2r)]/[4r{x_{gel}}^2(2-x_{gel})]$$

The expression reduces correctly to limiting cases. For $f(x_{gel}) = 0$, $x_{gel} = (1+2r)/(1+6r)$; for $f(x_{gel}) = 1$, $x_{gel} = 1$ (all $\mathbf{A_2B_2}$ monomers have one intramolecular cycle and convert into bifunctional monomers). Taking the experimental values of x_{gel} for $r = 1/3$ ($x_{gel} = 0.72$) and $r = 1$ ($x_{gel} = 0.57$), leads to $f(x_{gel}) = 0.56$ for $r = 1/3$ and $f(x_{gel}) = 0.53$ for $r = 1$.

Supporting Information Available: Figures showing ^{1}H and ^{13}C NMR spectra of the $\mathbf{A_2B_2}$ cross-linker. This material is available free of charge via the Internet at http://pubs.acs.org.

References and Notes

(1) Huisgen, R. In *1,3-Dipolar Cycloaddition Chemistry*; Padwa, A., Ed.; Wiley: New York, 1984; pp 1−176.
(2) Kolb, H. C.; Finn, M. G.; Sharpless, K. B. *Angew. Chem., Int. Ed.* **2001**, *40*, 2004–2021.
(3) Rostovtsev, V. V.; Green, L. G.; Fokin, V. V.; Sharpless, K. B. *Angew. Chem., Int. Ed.* **2002**, *41*, 2596–2599.
(4) Tornøe, C. W.; Christensen, C.; Meldal, M. *J. Org. Chem.* **2002**, *67*, 3057–3062.
(5) Binder, W. H.; Sachsenhofer, R. *Macromol. Rapid Commun.* **2008**, *29*, 952–981.
(6) Iha, R. K.; Wooley, K. L.; Nyström, A. M.; Burke, D. J.; Kade, M. J.; Hawker, C. J. *Chem. Rev.* **2009**, *109*, 5620–5686.
(7) Lutz, J.-F. *Angew. Chem., Int. Ed.* **2007**, *46*, 1018–1025.
(8) Carlmark, A.; Hawker, C.; Hult, A.; Malkoch, M. *Chem. Soc. Rev.* **2009**, *38*, 352–362.
(9) Binauld, S.; Hawker, C. J.; Fleury, E.; Drockenmuller, E. *Angew. Chem., Int. Ed.* **2009**, *48*, 6654–6658.
(10) Vogt, A. P.; Sumerlin, B. S. *Macromolecules* **2009**, *44*, 1–13.
(11) (a) Johnson, J. A.; Finn, M. G.; Koberstein, J. T.; Turro, N. J. *Macromol. Rapid Commun.* **2008**, *29*, 1052–1072. (b) Johnson, J. A.; Lewis, D. R.; Diaz, D. D.; Finn, M. G.; Koberstein, J. T.; Turro, N. J. *J. Am. Chem. Soc.* **2006**, *128*, 6564–6565.
(12) Malkoch, M.; Vestberg, R.; Gupta, N.; Mespouille, L.; Dubois, P.; Mason, A. F.; Hedrick, J. L.; Liao, Qi.; Frank, C. W.; Kingsbury, K.; Hawker, C. J. *Chem. Commun.* **2006**, *26*, 2774–2776.
(13) Polizzotti, B. D.; Fairbanks, B. D.; Anseth, K. S. *Biomacromolecules* **2008**, *9*, 1084–1087.
(14) Liu, S. Q.; Ee, P. L. R.; Ke, C. Y.; Hedrick, J. L.; Yang, Y. Y. *Biomaterials* **2009**, *30*, 1453–1461.
(15) Ossipov, D. A.; Hilborn, J. *Macromolecules* **2006**, *39*, 1709–1718.
(16) Crescenzi, V.; Cornelio, L.; Di Meo, C.; Nardecchia, S.; Lamanna, R. *Biomacromolecules* **2007**, *8*, 1844–1850.
(17) Xu, X.-D.; Chen, C.-S.; Wang, Z.-C.; Wang, G.-R.; Cheng, S.-X.; Zhang, X.-Z.; Zhuo, R.-X. *J. Polym. Sci., Part A* **2008**, *46*, 5263–5277.
(18) Xu, X.-D.; Chen, C.-S.; Bo, L.; Wang, Z.-C.; Cheng, S.-X.; Zhang, X.-Z.; Zhuo, R.-X. *Macromol. Rapid Commun.* **2009**, *30*, 157–164.
(19) Tizzotti, M.; Labeau, M.-P.; Hamaide, T.; Drockenmuller, E.; Charlot, A.; Fleury, E. *J. Polym. Sci., Part A* **2010**, *48*, 2733−2742.
(20) Reed, R., Jr. U.S. Patent 6,103,029, August 15, 2000.
(21) Katritzky, A. R.; Meher, N. K.; Hanci, S.; Gyanda, R.; Tala, S. R.; Mathai, S.; Duran, R. S.; Bernard, S.; Sabri, F.; Singh, S. K.; Doskocz, J.; Ciaramitaro, D. A. *J. Polym. Sci., Part A* **2008**, *46*, 238–256.
(22) Musa, O.; Sridhar, L.; Yuan-Huffman, Q. W., WO Patent 2008/048733, April 24, 2008.
(23) Diaz, D. D.; Punna, S.; Holzer, P.; McPherson, A. K.; Sharpless, K. B.; Fokin, V. V.; Finn, M. G. *J. Polym. Sci., Part A* **2004**, *42*, 4392–4403.
(24) Liu, Y.; Diaz, D. D.; Accurso, K.; Sharpless, B.; Fokin, V. V.; Finn, M. G. *J. Polym. Sci., Part A* **2007**, *45*, 5182–5189.
(25) Le Baut, N.; Diaz, D. D.; Punna, S.; Finn, M. G.; Brown, H. *Polymer* **2007**, *48*, 239–244.
(26) Wan, L. Q.; Luo, Y.; Xue, L.; Tian, J.; Hu, Y.; Qi, H.; Shen, X.; Huang, F.; Du, L.; Chen, X. *J. Appl. Polym. Sci.* **2007**, *104*, 1038–1042.
(27) Wan, L. Q.; Tian, J.; Huang, J.; Hu, Y.; Huang, F.; Du, L. *J. Appl. Polym. Sci.* **2007**, *106*, 2111–2116.
(28) Tian, J.; Wan, L. Q.; Huang, J.; Hu, Y.; Huang, F.; Du, L. *Polym. Adv. Technol.* **2007**, *18*, 556–561.
(29) Tian, J.; Wan, L. Q.; Huang, J.; Hu, Y.; Huang, F.; Du, L. *Polym. Bull.* **2008**, *60*, 457–465.
(30) Binauld, S.; Damiron, D.; Hamaide, T.; Pascault, J.-P.; Fleury, E.; Drockenmuller, E. *Chem. Commun.* **2008**, *35*, 4138–4140.
(31) Binauld, S.; Boisson, F.; Hamaide, T.; Pascault, J.-P.; Drockenmuller, E.; Fleury, E. *J. Polym Sci., Part A* **2008**, *46*, 5506–5517.
(32) Besset, C.; Binauld, S.; Ibert, M.; Fuertes, P.; Pascault, J.-P.; Fleury, E.; Bernard, J.; Drockenmuller, E. *Macromolecules* **2010**, *43*, 17–19.
(33) Fenouillot, F.; Rousseau, A.; Colomines, G.; Saint-Loup, R.; Pascault, J.-P. *Prog. Polym. Sci.* **2010**, *35*, 578–622.
(34) Winter, H. H.; Mours, M. *Adv. Polym. Sci.* **1997**, *134*, 135–234.
(35) Chambon, F.; Winter, H. H. *J. Rheol.* **1987**, *31*, 683–697.
(36) Pascault, J.-P.; Sautereau, H.; Verdu, J.; Williams, R. J. J. *Thermosetting Polymers*; Marcel Dekker: New York, 2002.
(37) Pascault, J. P.; Williams, R. J. J. *J. Polym. Sci., Part B* **1990**, *28*, 85–95.
(38) Williams, R. J. J. *Polymer Networks*, Stepto, R. F. T., Ed.; Blackie Academic and Professional: London, 1998, 93−124.
(39) Eloundou, J. P.; Gérard, J. F.; Harran, D.; Pascault, J. P. *Macromolecules* **1998**, *29*, 6917–6927.
(40) Stepto, R. F. T. *Polymer Networks*, Stepto, R. F. T., Ed.; Blackie Academic and Professional: London, 1998, 14−63.